jove

Experimental and Data Analysis Workflow for Soft Matter Nanoindentation

Giuseppe Ciccone[1], **Mariana Azevedo Gonzalez Oliva**[1], **Nelda Antonovaite**[2], **Ines Lüchtefeld**[3], **Manuel Salmeron-Sanchez**[1], **Massimo Vassalli**[1]

[1] Centre for the Cellular Microenvironment, James Watt School of Engineering, University of Glasgow [2] Optics 11 life [3] Laboratory of Biosensors and Bioelectronics, ETH Zürich

Corresponding Authors

Giuseppe Ciccone
g.ciccone.1@research.gla.ac.uk

Mariana Azevedo Gonzalez Oliva
m.azevedo-gonzalez-oliva.1@research.gla.ac.

Citation

Ciccone, G., Azevedo Gonzalez Oliva, M., Antonovaite, N., Lüchtefeld, I., Salmeron-Sanchez, M., Vassalli, M. Experimental and Data Analysis Workflow for Soft Matter Nanoindentation. *J. Vis. Exp.* (179), e63401, doi:10.3791/63401 (2022).

Date Published

January 18, 2022

DOI

10.3791/63401

URL

jove.com/video/63401

Abstract

Nanoindentation refers to a class of experimental techniques where a micrometric force probe is used to quantify the local mechanical properties of soft biomaterials and cells. This approach has gained a central role in the fields of mechanobiology, biomaterials design and tissue engineering, to obtain a proper mechanical characterization of soft materials with a resolution comparable to the size of single cells (μm). The most popular strategy to acquire such experimental data is to employ an atomic force microscope (AFM); while this instrument offers an unprecedented resolution in force (down to pN) and space (sub-nm), its usability is often limited by its complexity that prevents routine measurements of integral indicators of mechanical properties, such as Young's Modulus (*E*). A new generation of nanoindenters, such as those based on optical fiber sensing technology, has recently gained popularity for its ease of integration while allowing to apply sub-nN forces with μm spatial resolution, therefore being suitable to probe local mechanical properties of hydrogels and cells.

In this protocol, a step-by-step guide detailing the experimental procedure to acquire nanoindentation data on hydrogels and cells using a commercially available ferrule-top optical fiber sensing nanoindenter is presented. Whereas some steps are specific to the instrument used herein, the proposed protocol can be taken as a guide for other nanoindentation devices, granted some steps are adapted according to the manufacturer's guidelines. Further, a new open-source Python software equipped with a user-friendly graphical user interface for the analysis of nanoindentation data is presented, which allows for screening of incorrectly acquired curves, data filtering, computation of the contact point through different numerical procedures, the conventional computation of *E*, as well as a more advanced analysis particularly suited for single-cell nanoindentation data.

Introduction

The fundamental role of mechanics in biology is nowadays established[1,2]. From whole tissues to single cells, mechanical properties can inform about the pathophysiological state of the biomaterial under investigation[3,4]. For example, breast tissue affected by cancer is stiffer than healthy tissue, a concept that is the basis of the popular palpation test[5]. Notably, it has been recently shown that the coronavirus disease 2019 (COVID-19) caused by severe acute respiratory syndrome coronavirus 2 (SARS-CoV-2) is underlined by changes in the mechanical properties of blood cells, including decreased erythrocyte deformability and decreased lymphocyte and neutrophil stiffness as compared to blood cells from SARS-CoV-2-naïve individuals[6].

In general, the mechanics of cells and tissues are inherently intertwined: each tissue has specific mechanical properties that simultaneously influence and depend on those of the constituent cells and extracellular matrix (ECM)[5]. Because of this, strategies to study mechanics in biology often involve engineering substrates with physiologically relevant mechanical stimuli to elucidate cell behavior in response to those stimuli. For example, the seminal work by Engler and colleagues demonstrated that mesenchymal stem cell linage commitment is controlled by matrix elasticity, as studied on soft and stiff two-dimensional polyacrylamide (PAAm) hydrogels[7].

Many strategies to mechanically characterize the biomaterial under investigation exist, varying in spatial scale (i.e., local to bulk) and in the mode of deformation (e.g., axial vs shear), consequently yielding different information, which needs careful interpretation[3,8,9,10]. The mechanics of soft biomaterials is commonly expressed in terms of stiffness. However, stiffness depends on both material properties and geometry, whereas elastic moduli are fundamental properties of a material and are independent of the material's geometry[11]. As such, different elastic moduli are related to the stiffness of a given sample, and each elastic modulus encompasses the material's resistance to a specific mode of deformation (e.g., axial vs shear) under different boundary conditions (e.g., free expansion vs confinement)[11,12]. Nanoindentation experiments allow the quantification of mechanical properties through the *E* which is associated with uniaxial deformation (indentation) when the biomaterial is not laterally confined[10,11,12].

The most popular method to quantify *E* of biological systems at the microscale is AFM[13,14,15,16]. AFM is an extremely powerful tool with force resolution down to the pN level and spatial resolution down to the sub-nm scale. Further, AFM offers extreme flexibility in terms of coupling with complementary optical and mechanical tools, extending its capabilities to extract a wealth of information from the biomaterial under investigation[13]. Those attractive features, however, come with a barrier-to-entry represented by the complexity of the experimental set-up. AFM requires extensive training before users can acquire robust data, and its use for everyday mechanical characterization of biological materials is often unjustified, especially when its unique force and spatial resolutions are not required.

Because of this, a new class of nanoindenters has recently gained popularity due to their ease of use, while still offering AFM-comparable data with sub-nN force resolution and μm spatial resolution, reflecting forces exerted and

perceived by cells over relevant length scales[2]. Particularly, ferrule-top nanoindentation devices based on optical fiber sensing technology[17,18] have gained popularity among researchers active in the field of mechanobiology and beyond; and a wealth of works reporting the mechanical properties of biomaterials using these devices, including cells[19,20], hydrogels[8,21], and tissues[22,23] have been published. Despite the capabilities of these systems to probe local dynamic mechanical properties (i.e., storage and loss modulus), quasi-static experiments yielding *E* remain the most popular choice[8,19,20,21]. In brief, quasi-static nanoindentation experiments consists of indenting the sample with a constant speed up to a set-point defined either by a maximum displacement, force, or indentation depth, and recording both the force and the vertical position of the cantilever in so-called force-distance (*F-z*) curves. *F-z* curves are then converted into force-indentation (*F-δ*) curves through the identification of the contact point (CP), and fitted with an appropriate contact mechanics model (usually the Hertz model[13]) to compute *E*.

While the operation of ferrule-top nanoindenters resembles AFM measurements, there are specificities worth considering. In this work, a step-by-step guide to robustly acquire *F-z* curves from cells and tissue-mimicking hydrogels using a commercially available ferrule-top nanoindenter is provided, in order to encourage standardization of experimental procedures between research groups using this and other similar devices. In addition, advice on how to best prepare hydrogel samples and cells to perform nanoindentation experiments is given, together with troubleshooting tips along the experimental pathway.

Furthermore, much of the variability in nanoindentation results (i.e., *E* and its distribution) depends on the specific procedure used to analyze data, which is non-trivial. To address this issue, instructions for the use of a newly developed open-source software programmed in Python and equipped with a user-friendly graphical user interface (GUI) for batch analysis of *F-z* curves are provided. The software allows for fast data screening, filtering of data, computation of the CP through different numerical procedures, the conventional computation of *E*, as well a more advanced analysis named the elasticity spectra[24], allowing to estimate the cell's bulk Young's modulus, actin cortex's Young's modulus, and actin cortex's thickness. The software can be freely downloaded from GitHub and can be easily adapted to analyze data originating from other systems by adding an appropriate data parser. It is emphasized that this protocol can be used for other ferrule-top nanoindentation devices, and other nanoindentation devices in general, granted some steps are adapted according to the specific instrument's guidelines. The protocol is schematically summarized in **Figure 1**.

Protocol

1. Preparation of substrates/cells for nanoindentation measurements

1. Follow the steps given in the **Supplementary Protocol** for preparation of PAAm hydrogels/cells for nanoindentation experiments. The procedure is summarized in **Figure 2**.

   NOTE: PAAm hydrogels have been chosen as they are the most common hydrogels used within the field of mechanobiology. However, the protocol is equally applicable to any type of hydrogel[25] (see **Discussion**, modifications of the method).

2. Starting up the device, probe choice, and probe calibration

1. Follow the steps given in the **Supplementary Protocol** for starting up the device. For technical details on the operation of optical fiber ferrule-top nanoindenters, check these references[17,18].
2. Select the nanoindentation probe as described below.
   NOTE: All commercially available probes such as the ones used in this protocol are equipped with a spherical tip (**Figure 3A**). Therefore, the choice narrows down to two variables: cantilever's stiffness and tip radius (**Figure 3B**).
   1. Choose a cantilever's stiffness (*k* in N/m) that matches the expected sample stiffness for best results[15] (see **Figure 3C** and **Discussion**, critical steps in the protocol). For cells, select a probe with *k* in the range 0.01-0.09 N/m. For hydrogels, select a probe with *k* in the range 0.1-0.9 N/m, which yields optimal results for gels with expected *E* between a few kPa and 100 kPa (see **Representative Results**).
   2. Choose the tip radius (*R* in µm) according to the desired spatial resolution of the indentation process. For small cells such as Human Embryonic Kidney 293T (HEK293T) cells (average diameter of ~10-15 µm[26]) select a sphere with *R* = 3 µm. For hydrogels, select a sphere with *R* = 10-250 µm to probe the biomaterial's mechanical properties over a large contact area and avoid local heterogeneities.
   3. Consult **Figure 3C** and any additional manufacturer's guidelines to select the appropriate probe.
3. Once the probe has been selected, follow the steps in the **Supplementary Protocol** to mount it on the nanoindenter.

3. Probe calibration

NOTE: The following steps are specific to ferrule-top nanoindentation devices based on optical fiber sensing technology, and they are detailed for software version 3.4.1. For other nanoindentation devices, follow the steps recommended by the device manufacturer.

1. On the software's main window, click on **Initialize**. A calibration menu will appear. Enter the probe details (can be found on the side of the probe's box; *k* in N/m, *R* in µm, and the calibration factor in air) in the input boxes.
2. Prepare the calibration dish: a thick glass Petri dish with a flat bottom (see **Discussion**, critical steps in the protocol). Fill the dish with the same medium as the sample dish (this can also be air). Match the temperature of the medium with that of the sample.
3. Place the calibration dish under the probe. If required, slide out the probe from the nanoindenter's arm holder and hold it in one hand to make space for placement of the calibration dish. Slide back the probe into place.
4. Perform the next two steps for calibration in liquid. If measuring in air, use the provided polytetrafluoroethylene substrate for calibration and skip to step 5.
   1. Prewet the probe with a drop of 70% ethanol using a Pasteur pipette with the end of the pipette in light contact with the glass ferrule, for the drop to slide over the cantilever and spherical tip[27] (see **Discussion**, critical steps in the protocol).

2. Manually slide the nanoindenter's arm downwards until the probe is fully submerged, but still far away from the bottom of the Petri dish. If required, add more medium to the calibration dish. Wait 5 min so that equilibrium conditions are reached in the liquid.

5. In the software's **Initialize** menu, click on **Scan Wavelength**. The interferometer's screen will show a progress bar and the **Live Signal** window on the computer's software will display the pattern shown in **Figure S1A**, left. To check whether the optical scan was successful, navigate to the **Wavelength Scan** panel on the interferometer box. If successful, a sine wave should be visible (**Figure 1A**, right). See **Discussion** (troubleshooting of the method) if an error appears.

6. In the **Initialize** menu, click on **Find Surface**, which will progressively lower the probe until a set threshold in the cantilever's bending is reached. The probe stops moving when contact with the glass Petri dish is made.

7. Check whether the probe is in contact with the surface. Move the probe down by 1 µm using the *y* downwards arrow button on the software's main window. Observe the green signal (cantilever's deflection) in the **Live Window** of the software for changes in the baseline with each step, when the cantilever is in contact with the substrate (**Figure S1B**). If there is no change, the cantilever is not in contact (see next step).

8. Increase the **Threshold** value in the **Options** menu under the **Find Surface** tab from its default value of 0.01 by a step of 0.01 at a time and repeat the **Find Surface** step until in contact. Alternatively, bring down the probe to contact in small 1 µm steps until the green baseline starts shifting at each downwards step.

   NOTE: For the softest cantilevers (k = 0.025 Nm^{-1}), increase the **Threshold** value in the **Options** menu under the **Find Surface** tab *a priori* of performing step 6. Start from a threshold value of 0.06 or 0.07 and increase it up to 0.1 if necessary. This is because environmental noise will likely cause the cantilever to bend above the threshold prior to contact. For soft probes, decreasing the **Approach Speed (µm/s)** in the same menu also improves the procedure.

9. In the **Initialize** menu, click on **Calibrate**.

10. Check the **Live Signal** window of the software and make sure that both piezo's displacement and cantilever's deflection signals move up at the same time (**Figure S1C**).

    1. If there is a mismatch in time, the probe is not fully in contact with the glass. Move down the probe at steps of 1 µm until the baseline of the cantilever signal changes (see step 7) and repeat step 9.

    2. If the cantilever signal does not change at all during the **Calibrate** step, then the probe is far from the surface. Increase the contact threshold iteratively (see step 8) until the surface is found correctly and repeat calibration from the beginning starting with the wavelength scan.

11. When the calibration is complete, check the old and new calibration factors on the pop-up window displayed. If the new calibration factor is in the correct range, click on **Use New Factor**. If calibration fails, and the new factor is either NaN or is not in the expected range, see **Discussion** (troubleshooting of the method) for resolution.

    NOTE: The new factor should be ~*n* times lower than the one provided on the probe's box if the calibration

was performed in a liquid medium with refractive index *n* (*n* = 1.33 for water). If calibration was performed in air, then the new and old calibration factors should be approximately equal.

12. Check whether the demodulation circle has been correctly calibrated as follows. Navigate to the **Demodulation** tab on the interferometer desktop. Gently tap on the optical table or on the nanoindenter to induce enough noise. A white circle made up of discrete data points should approximately cover the red circle (**Figure S1D**).

13. If the white circle does not overlap with the red circle, or a warning appears on the interferometer's display, the demodulation circle needs recalibration. This can be done in two ways as described below.

    1. Continuously tap on the body of the nanoindenter to induce one full circle of noise and press the **Calibrate** button on the interferometer.

    2. Enter in contact with the glass substrate and press **Calibrate** from the **Initialize** menu of the software's main window. Do not save the calibration factor. At this point, check again and make sure the white circle overlaps with the red circle.

       NOTE: If the signal is not just slightly displaced from the demodulation circle but rather became very small or is not visible at all, it means that the cantilever is stuck to the optical fiber. Follow the troubleshooting advice for this problem (see **Discussion**, troubleshooting of the method) and repeat either steps 13.1 or 13.2. Once the cantilever gets back to its horizontal position (**Figure 3A**), the signal will recover to the demodulation circle.

14. Verify the calibration by performing an indentation on the glass substrate directly after the calibration as described below.

    1. Load or make an experiment file by clicking on **Configure Experiment** and add a **Find Surface** step and **Indentation** step. For the indentation step, use the default displacement mode settings and change the maximum displacement to the calibration distance (3,000 nm) to displace the probe against the stiff substrate.

    2. Click on **Run Experiment** and check the demodulation circle in the interferometer window. Check the white signal and make sure it is on top of the red circle during indentation.

    3. Check the results on the software's main window in the **Time Data** graph, and make sure the piezo's displacement (blue line) is equal to the cantilever's deflection (green line) as the indentation starts in contact and no material deformation is expected. If the signals are not parallel, see **Discussion** (troubleshooting of the method).

15. Change the local path in the calibration menu by setting the **Calibration Save Path** to an appropriate directory.

16. When the probe has been successfully calibrated, move the piezo up by 500 µm.

4. Measuring the Young's Modulus of soft materials

1. Nanoindentation of hydrogels

    1. Load the Petri dish containing the sample(s) on the microscope's stage and manually move the nanoindenter's probe to a desired *x-y* position above the sample.

2. Manually slide the probe in solution, taking care to leave 1-2 mm between the probe and the sample's surface at this stage. Wait 5 min for the probe to equilibrate in the medium.

3. Focus the *z* plane of the optical microscope so that the probe is clearly visible.

4. Perform a single indentation to tune the experimental parameters as described below.

    1. Configure a new experiment in the software's main window. Click on **Configure Experiment**, which will open a new window. Add a **Find Surface** step. All parameters of the **Find Surface** step can be changed in the **Options** menu of the software if required.

        NOTE: The **Find Surface** will lower the probe until the surface is found, and then it will retract the probe to a distance defined by **Z Above Surface (µm)**, above the sample's surface. If the selected cantilever is too stiff for the sample or the sample is sticky, after the step the probe is likely to still be in contact with the sample, which will result in a curve without a baseline (**Figure 4C**). To solve this problem, increase the **Z Above Surface (µm)**.

    2. Add an **Indentation** step. Select the **Profile** tab and click on **Displacement Control**. Leave the default indentation profile.

    3. Click on **Run Experiment** on the main software window. This will find the surface and perform a single indentation.If the single indentation does not look as expected, adjust the experimental parameters as outlined in **Figure 4** and **Discussion** (troubleshooting of the method).

5. Once the indentation looks as desired, configure the matrix scan so that a sufficient area of the sample will be indented. Click on **Configure Experiment**, add a **Find Surface** step with the previously determined experimental parameters and add a **Matrix Scan** step.

6. For flat hydrogels, configure a matrix scan containing 50-100 points (i.e., 5 x 10 or 10 x 10 in *x* and *y*) spaced at 10-100 µm (i.e., *dx* = *dy* = 10-100 µm). Click on **Use Stage Position** to start the matrix scan from the current stage position. Make sure the **Auto Find Surface** box is ticked to find the surface at each indentation using the set experimental parameters.

    1. To avoid oversampling, set the step size to at least twice the contact radius ($a = \sqrt{R\delta}$, where δ is the indentation depth).

    2. Set up the matrix scan profile in displacement control. Ensure that the profile does not violate the assumptions of the Hertz model (see **Discussion**, critical steps in the protocol).

    3. Leave the number of segments to 5, which is the default value, and use the default displacement profile. If necessary, change the displacement profile in terms of maximum displacement and time for each sloped segment, which will affect the maximum indentation depth and the strain rate, respectively. Do not exceed strain rates > 10 µm/s (see **Discussion**, limitations of the method).

    4. Enter a value for the approach speed, which determines how fast the probe is displaced toward the sample before contact. Match the

retraction speed to the approach speed (see note below).

NOTE: For soft cantilevers and noisy environments, an approach speed of 1,000-2,000 nm/s is recommended. For stiffer cantilevers and controlled environments, this can be increased.

5. Save the configured experiment in the desired **Experiment Path** and select a directory where the data will be saved in the **Save Path**, in the **General** tab of the **Configure Experiment** window. Click on **Run Experiment**.

7. Once the matrix scan is completed, raise the probe by 200-500 µm and move the probe to a different area of the sample sufficiently far away from the first area.

8. Repeat the experiment at least two times so that sufficient data is acquired on each sample (i.e., at least two matrix scans per sample, containing 50-100 curves each).

2. Nanoindentation of cells

1. Load the sample on the microscope as described above.

2. For single-cell indentation, focus the *z* plane so that both cells and probe are visible at 20x or 40x magnification, depending on cell size and spreading.

3. Move the probe above the cell to be indented.

4. Configure a new experiment in the software's main window. Click on **Configure Experiment**, which will open a new window. Add a **Find Surface** and **Indentation** step with default parameters in displacement mode.

5. Click on **Run Experiment**, which will find the surface and perform a single indentation. Check whether the indentation was successful. If the curve does not look as expected, adjust the experimental parameters (see **Figure 4** and **Discussion**, troubleshooting of the method).

6. If the indentation was successful, add a matrix scan to the experiment. Follow the steps given for hydrogels' nanoindentation experiments; configure the matrix scan so that the step size allows for a small area of the cell to be indented; 25 points spaced at 0.5-5 µm for HEK293T cells.

1. Depending on the cell size, adapt the matrix scan to ensure the tip does not indent outside the cell limit, i.e., doing a different map geometry or probing fewer points.

7. Click on **Run Experiment** and wait for it to be completed.

8. Once the matrix scan is completed, raise the probe out of contact (50 µm in the *z* plane).

9. Move the probe above a new cell and repeat the process (see **Discussion**, critical steps in the protocol).

3. Cleaning the probe and switching off the instrument

1. Follow the steps given in the **Supplementary Protocol** to clean the probe and switch off the nanoindentation device.

5. Data analysis

1. Downloading and installing the software

1. Follow the steps given in the **Supplementary Protocol** to download and install the software for data analysis[28,29].

2. Screening *F-z* curves and production of cleaned data set in JSON format

    1. Launch **prepare.py** from the command line on the lab computer as outlined in steps 2 to 3.

    2. If using a Windows computer, hold the shift key while right-clicking on the **NanoPrepare** folder and click on **Open PowerShell Window Here**. Type the **python prepare.py** command and press the **Enter** key. A GUI will pop up on your screen (**Figure S2**).

    3. If using a MacOS computer, right-click on the **NanoPrepare** folder and click on **New Terminal at Folder**. Type the **python3 prepare.py** command and press the **Enter** key, which will launch the GUI (**Figure S2**).

    4. Select the **O11NEW** data format from the drop-down list. If data is not loaded correctly, then relaunch the GUI and select **O11OLD**.

        NOTE: The **O11NEW** format works for data obtained using ferrule-top optical fiber sensing nanoindentation devices with software version 3.4.1. This format will also work for previous software versions, at least those belonging to nanoindenters installed in 2019-2020.

    5. Click on **Load Folder**. Select a folder containing the data to be analyzed-single matrix scan or multiple matrix scans. The top graph (**Raw Curves**) will be populated with the uploaded data set. To visualize a specific curve, click on it. This will highlight it in green and show it on the bottom graph (**Current Curve**).

    6. Clean the data set using the tabs present on the right part of the GUI as outlined below.

        1. Use the Segment button to select the correct segment to be analyzed, which is the forward segment of *F-z* curves. The specific number depends on the number of segments selected in the nanoindentation software when performing experiments.

        2. Use the **Crop 50 nm** button to crop the curves by 50 nm at the extreme left (if **L** is ticked), right (if **R** is ticked), or both sides (if both R and L are ticked). Click this button several times to crop as much as is required. Use this to remove artifacts present at the start/end of *F-z* curves.

        3. Inspect the **Cantilever** tab for the spring constant, tip geometry, and tip radius. Inspect the tab to ensure that the metadata has been read correctly.

        4. Use the **Screening** tab to set a force threshold that will discard all the curves that did not reach the given force. Discarded curves will be highlighted in red.

        5. Use the **Manual Toggle** button to manually remove curves that have not been correctly acquired. Remove any curves by clicking on the specific curve and selecting **OUT**, which will highlight the curve in red.

    7. Click on **Save JSON**. Enter an appropriate name for the cleaned data set, which is a single JSON file. Send the JSON file to the computer where the NanoAnalysis software was installed.

6. Formal data analysis

1. Launch the **nano.py** file from the command line by navigating to the **NanoAnalysis** folder and launching a terminal as previously explained. Type the **python nano.py** or **python3 nano.py** command (depending on the operating system) and press the **Enter** key. A GUI will pop up on your screen (**Figure S3**).

2. On the top left of the GUI, click on **Load Experiment** and select the JSON file. This will populate the file list and the **Raw Curves** graph showing the data set in terms of *F-z* curves. Both *F* and *z* axes are shown relative to the CP coordinates, which are computed in the background when loading the dataset (see the following note). In the **Stats** box, check the values of the three parameters: $N_{activated}$, N_{failed}, and $N_{excluded}$.

   NOTE: $N_{activated}$ represents the number of curves that will be analyzed in the subsequent Hertz/elasticity spectra analysis and appear in black in the **Raw Curves** graph. N_{failed} represents the number of curves on which a reliable CP could not be found and appear in blue in the graph. These curves will automatically be discarded in the subsequent analysis. Upon opening the software, some curves may be automatically moved to the failed set. This is because the CP is calculated upon opening the software with the default Threshold algorithm (see below). $N_{excluded}$ represents the curves that are manually selected to be excluded from the analysis and will appear in red in the graph (see below).

3. Check whether the number of failed, excluded, and activated curves is reasonable. Check the **Raw Curves** graph to visualize the curves.

4. To visualize a specific curve in more detail, click on it. This will highlight it in green and show it on the **Current Curve** graph. Once a single curve has been selected, the *R* and *k* parameters (which must be the same for all curves) will be populated in the **Stats** box of the GUI.

5. Change the status of a given curve using the **Toggle** box. Click on the specific curve you want to change the status of, and then click on either **Activated, Failed**, or **Excluded**. The count in the **Stats** box is automatically updated.

   NOTE: To change the view of the data set in the **Raw Curves** graph use the **View** box. Click on **All** to show all curves (i.e., activated, failed, and excluded in the respective colors). Click on **Failed** to show the activated and the failed curves and click on **Activated** to only show the activated curves. To reset the status of all curves between activated and excluded, click on **Activated** or **Excluded** in the **Reset** box.

6. Once the dataset has been further cleaned, follow the data analysis pipeline outlined below.

   1. Filter any noise present in the curves using the filters implemented in the GUI (**Filtering Box**), namely, a custom filter called Prominency filter, the Savitzky Golay[30,31] (SAVGOL) filter, and a smoothing filter based on computing the median of the data in a given window (median filter). See **Discussion** (critical steps in the protocol) for details on filters.

   2. Inspect the filtered curves in the **Current Curve** graph. The filtered curve is shown in black whereas the non-filtered version of the curve is shown in green.

      NOTE: It is advised to filter the data as little as possible to preserve features of the original

signal. Over filtering may smooth out any differences present in the data. Working with the prominency filter activated is enough for the Hertz analysis of nanoindentation data. If the data is particularly noisy, then a SAVGOL or median filters may be additionally applied.

3. Select an algorithm to find the CP. In the **Contact Point** box, choose one of a series of numerical procedures that have been implemented in the software, namely, the Goodness of Fit (GoF)[32], Ratio of Variances (RoV)[32], Second derivative[33], or Threshold[33]. See **Discussion**, critical steps in the protocol for details on the algorithms.

   NOTE: The CP is the point at which the probe comes into contact with the material and needs to be identified in order to convert *F-z* data into *F-δ* data (for soft materials, *δ* is finite and needs to be calculated). The selected algorithm will be applied to all active curves of the data set, and curves where the algorithm fails to locate the CP robustly will be moved to the failed set.

4. Adjust the algorithm's parameters to suit your dataset so that the CP is located correctly as detailed in the **Discussion**, critical steps in the protocol.To view where the CP has been found on a single curve, select the curve by clicking on it and click on **Inspect**. Check the pop-up window that appears to identify where the CP has been located.

5. Check whether the red line that appears, which is the parameter the algorithm computed in the selected region of interest, has a maximum or minimum value that corresponds to the location of the CP (e.g., for the GoF, the parameter is the R^2). Repeat this process for all curves if needed.

   NOTE: The axes of the pop-up are in absolute coordinates so that the location of the CP can be shown. Conversely, the axes of the **Raw Curves** and **Current Curve** graph are shown relative to the CP, i.e., the location of the CP is (0,0).

6. Click on **Hertz Analysis**. This will generate three graphs described below.

   1. Check individual *F-δ* curves in the dataset together with the average Hertz fit (red dashed line). Adjust the indentation in nm up to which the Hertz model is fitted in the **Results** box under **Max Indentation (nm)**. Set it to a maximum of ~10% of *R* for the Hertz model to be valid (see **Discussion**, critical steps in the protocol).

   2. Check the average *F-δ* curve with error band showing one standard deviation (SD) together with the average Hertz fit (red dashed line). Visualize the average Hertz fit on the **Raw Curves** graph for reference and the Hertz fit for each curve on the **Current Curve**.

   3. Check the scatter plot of *E* originating from fitting the Hertz model to each individual curve.

7. Click on either the file name, *F-z* curve, *F-δ* curve, or a point on the scatter plot to highlight the curve in each plot. If a data point in the scatter plot appears to lie outside the distribution of the data, click on it and inspect the curve to which it belongs. Verify that the CP has been located correctly by clicking on the **Inspect** button. Exclude the curve from the analysis if necessary.

8. Inspect the **Results** box for the computed mean E and its SD ($E_Y \pm \sigma$) and make sure they are reasonable for the given experiment.

9. In the **Save** box, click on **Hertz**. In the pop-up window, enter file name and directory. Once done, click on **Save**. A .tsv file will be created. Open the .tsv file in any additional software of preference and use the values for statistical analysis and further plotting.
NOTE: The file contains the E obtained from each curve and the mean E and its SD. Additionally, the file contains metadata associated with the analysis, including the number of curves analyzed, R, k, and the maximum indentation used for the Hertz model.

10. This step is optional. Click on **Average F-Ind** to export the average force and the average indentation, together with one SD in the force.

11. For cell nanoindentation data, click on **Elasticity Spectra Analysis** (see **Representative Results** and **Discussion**). Inspect the two plots produced, namely, E as a function of the indentation depth ($E(\delta)$) for each curve, and the average $E(\delta)$ with error band showing one SD (solid red line and shaded area) fitted by a model (black dashed line), which allows to estimate the cell's actin cortex's Young's modulus, the cell's bulk Young's modulus, and the actin cortex's thickness. Additionally, check the average $E(\delta)$ in the top graph in red.

12. Make sure the **Interpolate** box is checked, which ensures the derivative needed to perform the elasticity spectra analysis is computed on the interpolated signal (see **Representative Results**).

13. Inspect the **Results** box, reporting the cortex's Young's modulus ($E_0 \pm \sigma$), the cell's bulk Young's modulus ($E_b \pm \sigma$), and the cortex thickness ($d_0 \pm \sigma$).
NOTE: The average elasticity spectra may appear noisy at first, with prominent sinusoidal oscillations. As a result, equation (3) may not be fitted correctly. If this is the case, iteratively increasing the window length of the smoothing SAVGOL filter[34] solves this issue.

14. Once the analysis is finished, click on **ES** in the **Save** box. This will export a .tsv file in the specified directory, containing the average elasticity as a function of the average indentation depth and contact radius, the metadata associated with the experiment (see above), and the estimated model parameters explained above. Finally, the average elasticity disregarding the dependency on δ and its SD, are also reported.

15. Close the software and input the saved results in any other software of preference to further plot the data and perform statistical analysis.

16. This step is optional: Export graphs from the GUI by right-clicking on the graph and selecting **Export**. Export the graph in .svg, so that parameters such as font, font size, line style, etc. can be edited in another software of choice.
NOTE: Custom CP algorithms and filters can be programmed and added to the already existing ones. See **Supplementary Note 1** for details.

Representative Results

Following the protocol, a set of F-z curves is obtained. The dataset will most likely contain good curves, and curves to

be discarded before continuing with the analysis. In general, curves should be discarded if their shape is different from the one shown in **Figure 4A**. **Figure 5AI** shows a dataset of ~100 curves obtained on a soft PAAm hydrogel of expected *E* 0.8 KPa[35] uploaded in the NanoPrepare GUI. Most curves present a clear, flat baseline, a transition region, and a sloped region that is proportional to the apparent stiffness of the material[13]. However, a minority of curves show alterations from the shape shown in **Figure 4A**, such as the absence of a baseline, missed contact, or a sloped baseline. These curves can be easily removed from the dataset using NanoPrepare (**Figure 5AII**, red curves), and a clean dataset saved in the standard JSON format (**Figure 5AIII**). The clean dataset is uploaded in NanoAnalysis (**Figure 5BIV**), which has been designed so that it batch processes all curves. This means each step of the workflow is applied to the whole dataset. After being uploaded, curves can be filtered to remove random noise using one or more filters described in the **Discussion**, critical steps in the protocol (**Figure 5BV**). The CP is then located using one of the algorithms implemented in the software and detailed in the **Discussion**, critical steps in the protocol (**Figure 5BVI**). Once the CP has been identified, *F-z* data is converted into *F-δ* data. Because the software has been designed to primarily analyze data from ferrule-top nanoindentation devices based on optical fiber sensing, which use probes having a spherical tip, the Hertz analysis is based on the Hertz model approximating the contact between a sphere of radius *R* and an infinitely extended linear elastic homogeneous isotropic (LEHI) half space[13]:

$$F = \frac{4}{3}\frac{E}{(1-\nu^2)}\delta^{\frac{3}{2}}R^{\frac{1}{2}} \qquad (1)$$

where *F* is the force, *δ* is the indentation, *E* is Young's Modulus, and *v* is the Poisson's ratio, taken as 0.5 assuming incompressibility. By fitting *F-δ* curves with equation (1), *E* can be therefore estimated (see **Discussion**-critical steps in the protocol-for assumptions of the Hertz model) (**Figure 5BVII**).

In addition to the Hertz analysis, the software can perform a more advanced analysis, namely, the elasticity spectra, which is particularly useful for cell nanoindentation data; and can also be used as a tool to estimate the influence of the underlying substrate on the mechanical properties obtained via the Hertz model. Below, the approach is briefly summarized. Full details can be found in the original publication[24].

Starting from the Oliver-Pharr model[36], which describes the indentation of an axisymmetric punch of arbitrary geometry and an elastic half space, one can derive *E*(*δ*) for the specific case of a spherical indenter. Taking *v* as 0.5, *E*(*δ*) has the form[24]:

$$E(\delta) = \frac{3}{8}\frac{1}{\delta\sqrt{R}}\frac{dF}{d\delta} \qquad (2)$$

Computing *E*(*δ*) for each *F-δ* curve using equation (2) yields a set of curves, namely, the elasticity spectra (ES). By taking the average of all curves in the data set, the average ES is obtained (**Figure 5BVIII**, red solid line). The average ES is a useful tool because it provides information on how *E* varies with *δ* in the dataset. In the specific case of cell nanoindentation experiments, the thickness of the cell is not known *a priori*, which means that choosing an appropriate fitting range for the Hertz analysis is somewhat arbitrary. By using the average ES, substrate effects on the apparent *E*(*δ*) become evident, which means the tool can be used to select an appropriate fitting range, corresponding to the point where *E*(*δ*) starts increasing after its decay. Further, it has been previously demonstrated and computationally

and experimentally validated that a simple bilayer model is effective in the estimation of the actin cortex's thickness (d_0), the actin cortex's Young's modulus (E_0), and the cell's bulk Young's modulus (E_b)[24]. The model describes the cell as a bilayer, with an outermost layer of thickness d_0 and modulus E_0, and an inner layer of infinite thickness with elastic modulus $E_b<E_0$:

$$E(\delta) = E_b + (E_0 - E_b)e^{-\left(\frac{\Lambda\sqrt{R\delta}}{d_0}\right)} \quad (3)$$

where R is the tip's radius and Λ is a phenomenological parameter, which was determined to be 1.74 from finite element analysis simulations[24]. This procedure has been implemented in the NanoAnalysis software, which allows to fit the average ES with equation (3) to obtain an estimate of E_0, E_b, and d_0 (**Figure 5BVIII**, black dashed line). For full methodological details, refer to the original publication[24].

To demonstrate the viability of the protocol, the elasticity of PAAm hydrogels of known E (measured by AFM)[35] were prepared and tested using the procedure suggested in Part 1 of the protocol. For each gel, two stiffness maps in two different areas of the sample were acquired using a commercial ferrule-top nanoindenter equipped with a tip having R = 52 µm and k = 0.46 N/m. Each map consisted of 50 indentations performed in displacement control, and the step size in x and y was set to 20 µm to avoid oversampling. **Figure 6A** shows the average F-δ curve together with the average Hertz model for a soft PAAm hydrogel (expected E 0.8 kPa) and a stiff PAAm hydrogel (expected E 8 kPa)[35]. By performing the Hertz analysis through the NanoAnalysis software and plotting individual values of E, the expected E was retrieved for both hydrogels (**Figure 6B**).

Further, nanoindentation experiments on HEK293T cells were performed. Six individual cells were indented by performing a matrix scan with x and y step size set to 0.5 µm on each cell and acquiring a minimum of 25 curves on each cell. This resulted in the analyzed dataset containing ~200 curves. The selected probe had R = 3.5 µm and k =0.02 N/m.

Figure 7A shows the average Hertz curve and the corresponding average Hertz model, plotted using the mean E obtained from fitting equation (1) to each individual curve in NanoAnalysis up to an indentation of 200 nm. E was found to be 915 ± 633 Pa (mean ± SD), which is in accordance with values reported in the literature[24]. Despite its wide use, the Hertz model does not fully capture the evolution of the force with increasing indentation depth for cell nanoindentation experiments (**Figure 7A**). Because of this, the ES is a particularly suitable tool to study the mechanical properties of single cells.

Figure 7B shows the average ES, together with equation (3) fitted up to an indentation of 200 nm. The average ES starts increasing at an indentation depth of ~200 nm, which indicates the contribution of the substrate to the probed apparent E (**Figure S4**). Because of this, 200 nm was chosen as the fitting range for both the Hertz model (**Figure 7A**) and the bilayer model (**Figure 7B**). Fitting equation (3) to the average ES allowed to extract important information, which would otherwise remain inaccessible from simple nanoindentation experiments analyzed using the Hertz model. Specifically, the actin cortex's modulus E_0 was estimated to be 5.794 ± 0.095 kPa, the actin cortex's thickness d_0 was found to be 311 ± 3 nm and the bulk modulus E_b was found to be 0.539 ± 0.002 kPa (mean ± SD). All values are in accordance with previous experiments performed using AFM on the same cell type[24], and with values that have been

reported in the literature[37,38]. Specifically, the actin cortex is expected to be between 300-400 nm for adherent cells[37], and up to 10 times stiffer than the bulk of the cell[38].

Regardless of the bilayer model, a direct comparison between results obtained with the standard Hertz model and the ES approach is given in **Figure 7C**, which reveals overlapping distributions with comparable means.

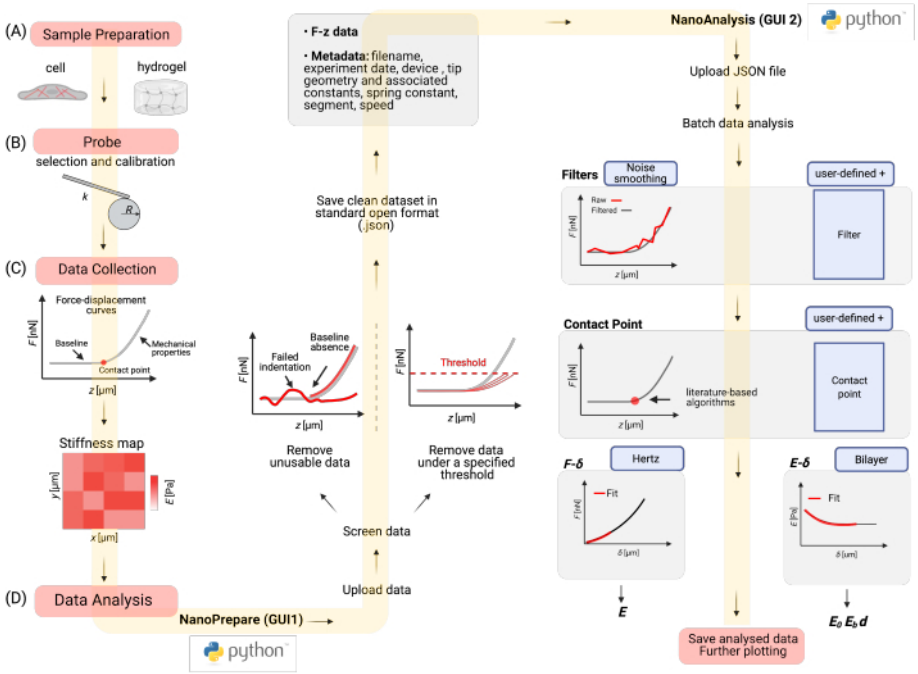

Figure 1: Protocol overview. The protocol consists of the following parts: (**A**) Part 1: Preparing the sample (either hydrogels or cells) for nanoindentation experiments. (**B**) Part 2: Choosing the right probe and calibrating the probe. (**C**) Part 3: Performing nanoindentation experiments by acquiring stiffness maps on the sample. (**D**) Part 4: Analyzing the data, which consists of i) cleaning the acquired dataset through the first GUI (NanoPrepare) and saving the cleaned dataset and associated metadata as a standard JSON file; and ii) analyzing the cleaned dataset in the second GUI (NanoAnalysis), which consists of data filtering, CP identification, and model fitting to estimate Young's modulus *E* of the sample. Results are saved for further plotting and statistical analysis, which can be performed in any software of choice. Created with Biorender.com. Please click here to view a larger version of this figure.

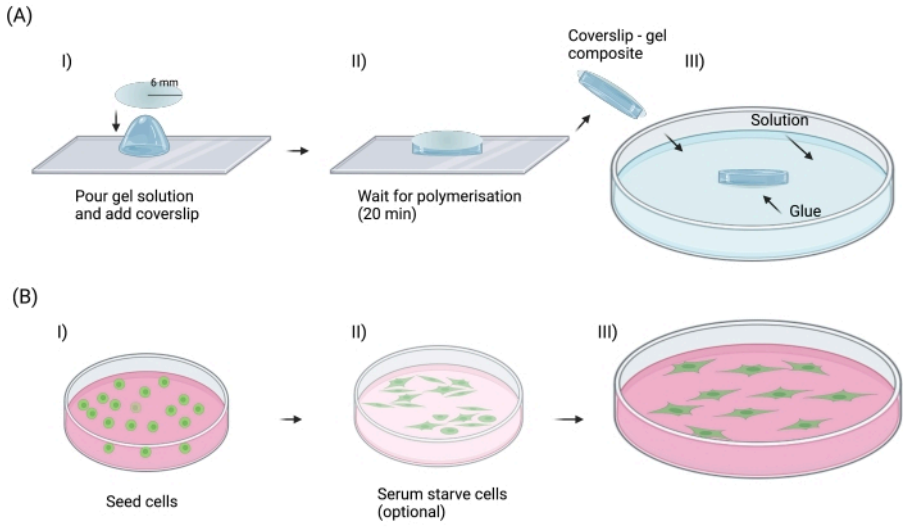

Figure 2: Sample preparation. (**A**) Steps suggested to prepare flat PAAm hydrogels for nanoindentation experiments. These are: I) pouring the hydrogel solution onto a hydrophobic glass slide and covering it with a silanized coverslip; II) waiting for 20 min for polymerization to occur and peeling off the coverslip-gel composite from the glass slide; and III) attaching the coverslip-gel composite to a Petri dish and adding appropriate solution (purified water in the context of this protocol) for nanoindentation experiments. The same rationale can be adapted and applied to any other type of hydrogel. (**B**) Steps suggested to prepare cells for nanoindentation experiments. These are: I) seeding cells and waiting for cell adhesion; II) serum starving the cells to synch the cell population in terms of the cell cycle (optional); and III) waiting for cells to be in an adhered state at desired confluency before starting nanoindentation experiments. Created with Biorender.com. Please click here to view a larger version of this figure.

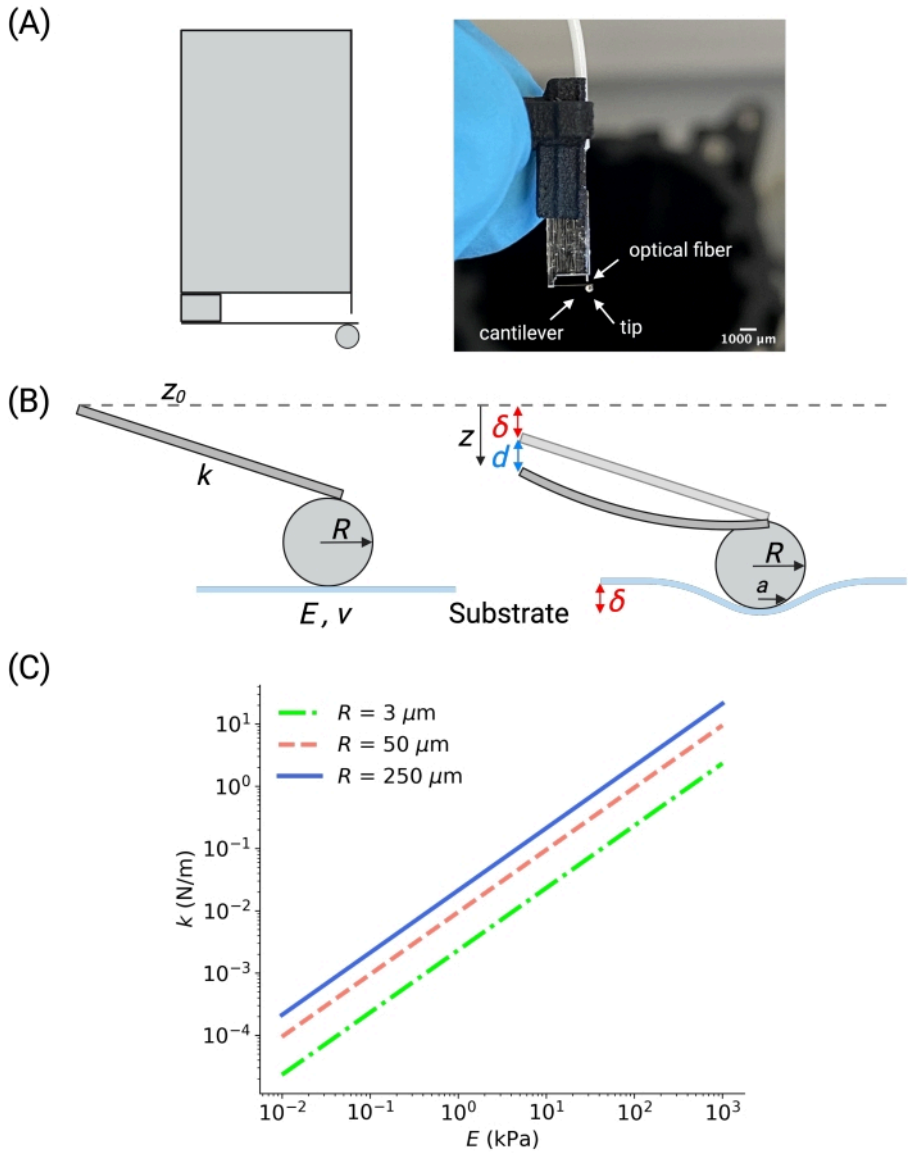

Figure 3: Nanoindentation probe overview and selection. (**A**) Schematic of ferrule-top probe (left) and picture of a ferrule-top probe with the spherical tip of radius 250 µm (right). All components are labeled in the photo. (**B**) Enlarged schematic of the cantilever and the spherical tip. The cantilever is treated as a Hookean spring of elastic constant *k* (shown at an angle for representation purposes). The tip is defined by its radius, *R*. When the sample is indented, the probe is displaced by an amount *z* from its reference position z_0, which results in the cantilever bending *d* from its reference bending d_0. A force of $F = k (d - d_0)$ is applied to the sample, which results in an indentation $\delta = (z - z_0) - (d - d_0)$. (**C**) Cantilever's stiffness *k* should be chosen according to the expected elasticity of the substrate. The plot was obtained considering Hertzian contact with an indentation of 1 µm, assuming that the energy is equally shared between the cantilever's bending and the substrate's

indentation (i.e., $d = \delta$). The larger the tip radius, the stiffer the cantilever should be to reach the same indentation for a substrate with a given E. Please click here to view a larger version of this figure.

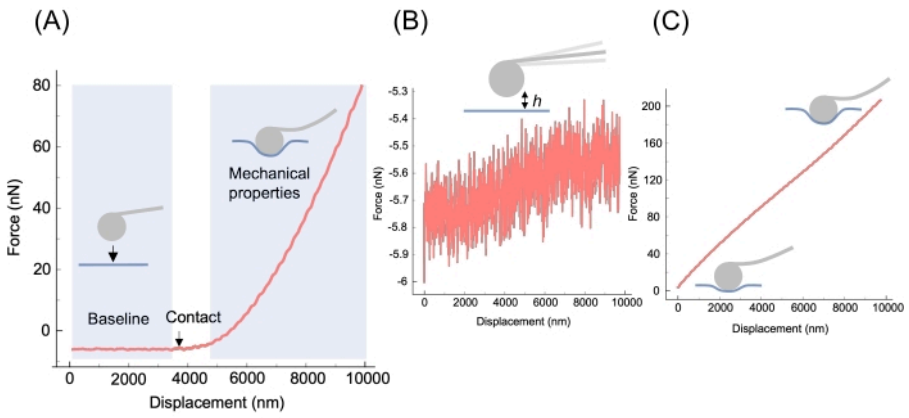

Figure 4: Morphological characteristics of *F-z* curves. (**A**) A successful experiment results in the approach segment of an *F-z* curve having a clear baseline (tip approaching the sample but not in contact); a transition region where the tip first contacts the sample; and a region where the force increases with the displacement, where the tip is progressively indenting the sample. The slope of this region is proportional to the apparent stiffness of the material[13], meaning that curves belonging to stiff biomaterials (e.g., highly crosslinked gels) will be steeper than those belonging to softer biomaterials (e.g., weakly crosslinked gels and cells). (**B**) An approach curve where the tip never entered contact with the sample. See troubleshooting of the method in the **Discussion** for resolution. (**C**) An approach curve where the tip started in contact with the sample. See troubleshooting of the method in the **Discussion** for resolution. The data shown is from an experiment performed on a soft PAAm hydrogel of expected E 0.8 kPa[35]. Please click here to view a larger version of this figure.

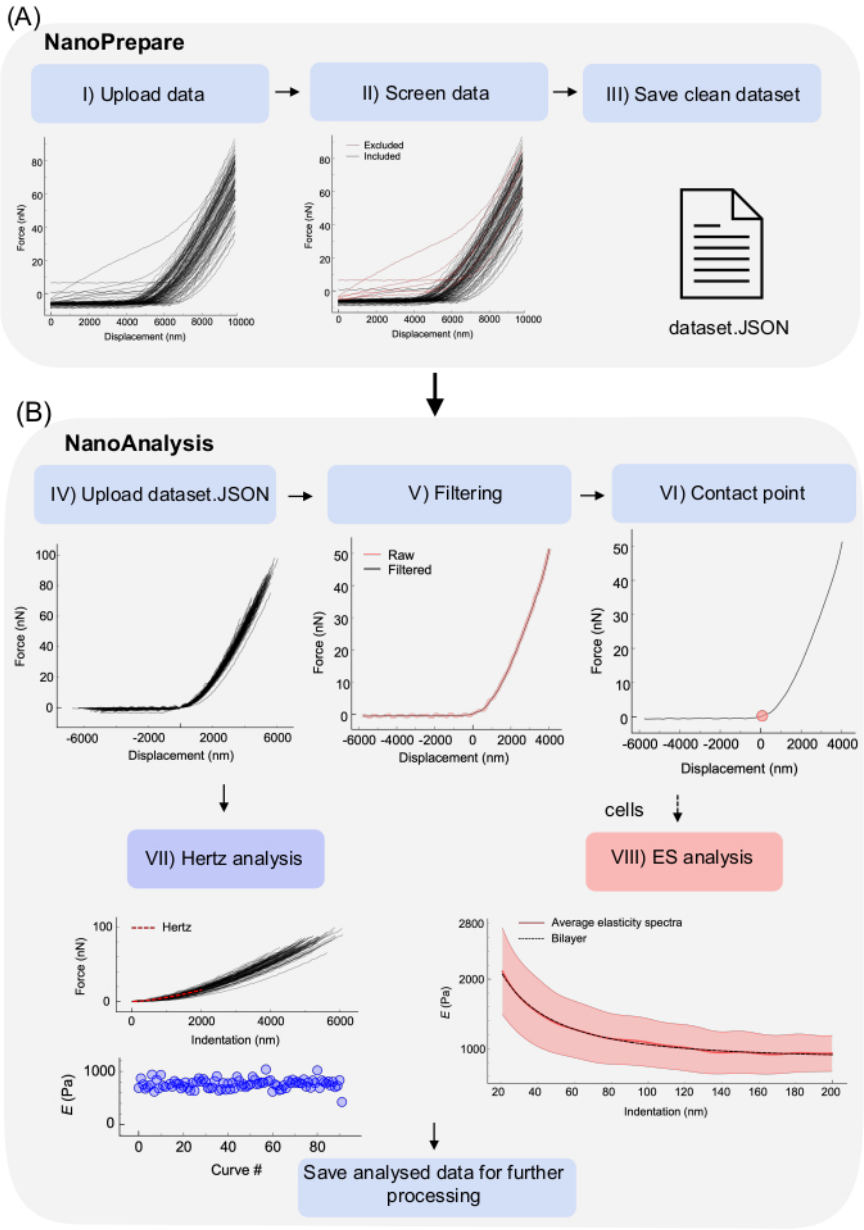

Figure 5: Data analysis workflow using the Python GUIs. (**A**) An example dataset of *F-z* curves acquired using a commercially available ferrule-top nanoindenter on a soft PAAm hydrogel (expected *E* 0.8 kPa[35]) was uploaded in NanoPrepare. Curves that do not follow the shape described in **Figure 4A** are excluded from the dataset, and the clean dataset and associated metadata are saved as a standard JSON file. (**B**) The clean dataset is uploaded in the second GUI (NanoAnalysis) where curves can be filtered by applying one or more filters to remove noise (see **Discussion**, critical steps in the protocol). Further, a CP algorithm is selected to automatically locate the CP for all curves (see **Discussion**, critical steps in the protocol). The Hertz analysis is then performed, yielding a *F-δ* curve for each indentation, which is fitted with the Hertz model to yield a scatter plot of *E*. The obtained results can be saved for further plotting. For cells, an additional

analysis called the elasticity spectra[24] can be performed. All graphs shown were directly exported from both NanoPrepare and NanoAnalysis GUIs. Details for each step of the workflow are given in the main text. Please click here to view a larger version of this figure.

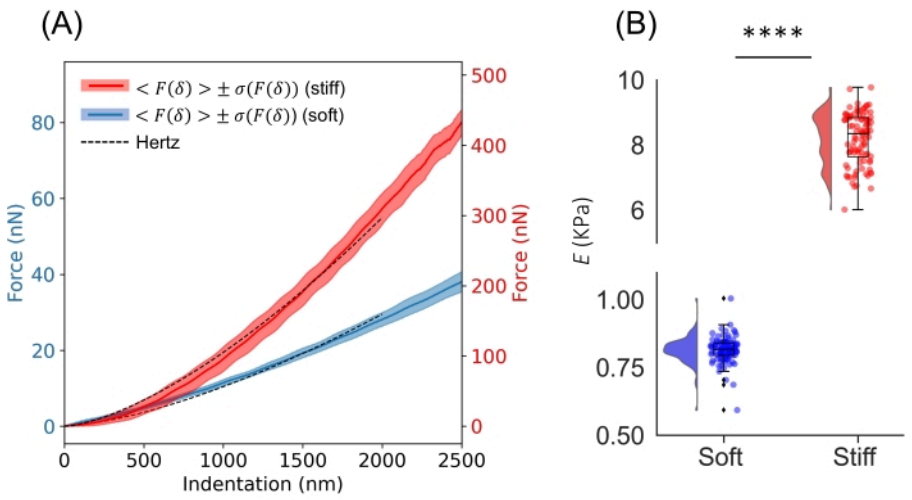

Figure 6: Elasticity of PAAm hydrogels. (**A**) Average *F-δ* curve from a set of ~100 curves acquired on a soft PAAm hydrogel (expected *E* 0.8 kPa[35]) and a stiff PAAm hydrogel (expected *E* 8 kPa[35]). Solid lines show the mean and shaded band shows one SD. The dashed line shows the Hertz model plotted using the average *E* from the NanoAnalysis software, obtained by fitting the Hertz model to each curve up to a maximum indentation of 2,000 nm (~4% of *R, R* = 52 µm, *k* = 0.46 N/m). Curves were smoothed using the prominecy filter with default parameters, and the CP was identified using the RoV algorithm[32]. (**B**) Individual values of *E* obtained from the analysis performed in NanoAnalysis plotted for statistical comparison. The raincloud plot was obtained using the Python module described in reference[39]. **** $p < 0.0001$, two-tailed unpaired *t*-test, α=0.05. Please click here to view a larger version of this figure.

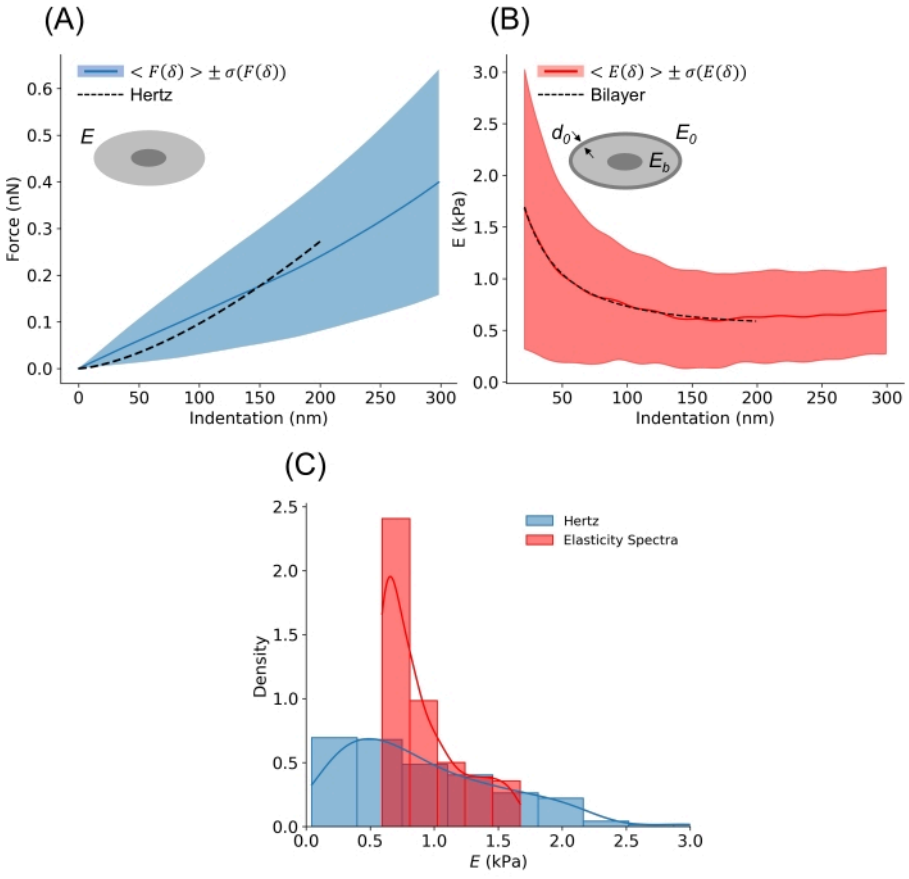

Figure 7: Elasticity of HEK293T cells. (**A**) Average *F-δ* curve from a set of ~200 curves acquired on six individual HEK293T cells. The solid blue line shows the mean and the shaded band shows one SD. The dashed line shows the Hertz model plotted using the average *E* computed using the NanoAnalysis software, obtained by fitting the Hertz model to each curve up to a maximum indentation of 200 nm (~6% of *R, R* = 3.5 µm, *k* = 0.02 N/m). Curves were smoothed using the prominecy filter with default parameters and a SAVGOL filter[34] with order 3 and window length 80 nm, and the CP was identified using the Threshold algorithm[33]. Using the Hertz model, the cell is treated as a homogeneous sphere with Young's Modulus *E,* as schematically shown in the inset (the nucleus is depicted for pictorial purposes). (**B**) Average elasticity spectra computed on the same data set described in (A). The solid red line shows the mean and the shaded band shows one SD. By fitting a bilayer model to the average elasticity spectra, estimations of E_0, E_b, and d_0 are computed. For the dataset shown: E_0 = 5.79 ± 0.09 kPa, E_b = 0.539 ± 0.002 kPa and d_0 = 311 ± 3 nm (mean ± SD). (**C**) Comparison between the Hertz model and the elasticity spectra approach in terms of *E* distribution. For the elasticity spectra, the distribution represents the values of *E* from the average elasticity spectra, regardless of indentation depth (up to a maximum indentation of 200 nm). The continuous lines superimposed on the histograms are Gaussian kernel density estimates of the underlying distributions.

E = 915 ± 633 Pa (Hertz) and E = 890 ± 297 Pa (elasticity spectra) (mean ± SD). Please click here to view a larger version of this figure.

Figure S1: Calibration Procedure. (**A**) Successful wavelength scan. The cantilever's deflection and piezo's displacement signals during the wavelength scan (left). The sinusoidal wave on the interferometer's screen at the end of the wavelength scan (right). (**B**) Find surface procedure. cantilever's deflection and piezo's displacement signals as the probe is lowered in 1 µm steps after contact with a stiff substrate. (**C**) Geometrical factor calibration. During indentation of a stiff substrate, the cantilever's deflection follows the cantilever's displacement (green and blue lines, respectively). The indentation should be approximately zero (red line). If the deflection lags the displacement in time (green dashed line), the probe is not fully in contact with the stiff substrate. (**D**) Demodulation signal. The demodulation signal on the interferometer's screen at the end of the calibration procedure (left) and when tapping on the nanoindenter (right). Please click here to download this File.

Figure S2: NanoPrepare GUI. Screenshots of the NanoPrepare GUI. Details on the functionality of each widget are given in the main **Protocol** and the **Discussion**. Please click here to download this File.

Figure S3: NanoAnalysis GUI. Screenshots of the NanoAnalysis GUI. Details on the functionality of each widget are given in the main **Protocol** and the **Discussion**. Please click here to download this File.

Supplementary Note 1: Adding custom filters and CP algorithms to the NanoAnalysis software. Please click here to download this File.

Supplementary Protocol. Please click here to download this File.

Figure S4: Depth dependency of average elasticity spectra. The plot shows the average elasticity spectra $\langle E(\delta) \rangle$ (solid red line) together with one SD $(\sigma(E(\delta))$. After an initial decay, the average elasticity spectra start increasing, which is mainly associated with the effects of the stiff underlying substrate on the probed apparent elastic modulus. The maximum indentation depth used to fit the Hertz model to F-δ curves, and the decay model to the average elasticity spectra should be chosen so that the underlying substrate does not affect the results (Fit range). Please click here to download this File.

Discussion

This protocol shows how to robustly acquire force spectroscopy nanoindentation data using a commercially available ferrule-top nanoindenter on both hydrogels and single cells. In addition, instructions for the use of an open-source software programmed in Python comprising a precise workflow for the analysis of nanoindentation data are provided.

Critical steps in the protocol

The following steps have been identified to be of particular importance when following this protocol.

Sample preparation

It is crucial that before initiating measurements, the sample is prepared with the restraints of the measurement in mind. That is, the sample must be adhered to a surface and be as flat as possible. This is especially important when

preparing samples that do not naturally adhere to surfaces as cells do, such as hydrogels. Firstly, the sample must not float in solution as this will interfere with measurements and potentially damage the probe. For this, chemical functionalization of a coverslip is recommended, so that the hydrogel can be polymerized adhered to a surface, which can later be glued to a Petri dish while submerged. Moreover, the sample's surface must be as flat as possible to ensure coherent surface detection by the probe and avoid damaging the probe while moving in *x* and *y* during a matrix scan. The hydrogel solution can be polymerized on a hydrophobic glass slide, which makes the resulting hydrogel flat without adhering to it. If these considerations are not followed, it will be difficult to obtain clean *F-z* data.

In the case of cell preparation, it is best to indent cells with similar morphology to improve data homogeneity. In the event that cells grow in a heterogeneous population, a serum starvation step can be introduced pre-measurement, to aid cell cycle synchronization and, therefore, remove potential experimental confounders[40,41]. In the case of non-adherent cells or organoid cultures, one must perform extra steps to ensure stability and adherence of the biological sample while measurements are being performed. Extra steps might include chemically binding cells to culture plates or using tissue adhesives that are now widely commercially available.

Nanoindentation experiments

It is important that a cantilever with the right *k* is chosen depending on the sample's expected *E*[15]. This is because if the cantilever is too stiff, the sample will be indented but no significant cantilever bending will occur. Conversely, if the cantilever is too soft with respect to the sample, the cantilever will excessively bend with minimal indentation. Both instances will result in the miscalculation of *E* in the subsequent analysis.

For probe calibration, the probe must be wet prior to insertion into the calibration dish to minimize surface tension when encountering the liquid of the calibration dish. Not doing so may cause the trapping of air bubbles or push the cantilever against the optical fiber. This can also result in the probe being damaged.

The use of a thick glass Petri dish is recommended for calibration. Glass is infinitely stiff compared to the cantilever, which allows accurate calibration of the cantilever's *k* while indenting the glass. Further, the weight of the glass ensures a stable substrate that is more robust against noise (e.g., airflow and acoustic vibrations) compared to a lighter plastic Petri dish. The calibration performs a linearization procedure of the interferometric signal measured at the detector (V/t), which means the signal will be converted into linear cantilever bending (µm/t) using the unit circle (demodulation circle) as a linearization tool[18]. The deflection sensitivity (µm/V) is set by default in the interferometer and used to convert V to µm. During this procedure, the calibration factor is also determined, which originates from the mismatch in position between the spherical tip and the fiber position where the signal read-out occurs (**Figure 3A**). By indenting on a stiff substrate-like glass, the deflection measured by the fiber is approximately the same as the distance displaced by the piezo, which means the indentation depth is approximately zero. Taking their ratio yields the calibration factor. It is important that the calibration of the instrument is performed correctly, and that all checks are satisfied before continuing to acquire *F-z* data.

When configuring an indentation profile, it is useful to keep in mind the assumptions of the Hertz model, which will be

used later to analyze the data. The Hertz model is derived assuming that the sample is a LEHI infinitely extended half-space, which results in the following practical consequences: i) applied strains should not exceed 20% (as a rule of thumb, δ should not exceed 10% of the tip's R) and ii) δ should be less than 10% of the sample thickness, and small compared to the other sample's dimensions[13].

The maximum displacement (or indentation depth/force depending on the operation mode) can be adjusted depending on the resulting δ, and whether surface or bulk mechanical properties are desired. If the sample has been indented to a slightly larger δ, the Hertz model can still be fitted up to a maximum δ which lies within its assumptions in the NanoAnalysis software, and the average ES used to estimate this range (see **Representative Results**).

For cell nanoindentation experiments, it is challenging to perform multiple matrix scans on the same cell. However, if the cell is large enough, it may be possible to find another suitable region and repeat the procedure on the same cell, for example, an experiment where the user wants to detect differences in the mechanical properties of a certain region of the cell compared to another. Usually, a map per cell is performed, and a minimum of five cells are indented per biological condition. It is advisable to repeat the experiment at least three times so that sufficient data is acquired on each sample (i.e., three replicates for each biological condition).

Critically, acquired curves should present a flat baseline, a transition region, and a sloped region. Curves that do not present a baseline cannot be later analyzed due to uncertainty on the location of the CP. If curves deviate from the shape shown in **Figure 4A**, the contact threshold should be optimized before continuing with the experiment (see troubleshooting of the method below).

Sufficient data should be acquired to ensure statistically robust results, given the nature of the technique, which probes mechanical properties locally.

Data analysis

The software described in this protocol is routinely adopted to analyze nanoindentation data and it has been used to obtain results published in several peer-reviewed journals (e.g., nanoindentation of hydrogels[8,21], nanoindentation of cells[24,42]). Analysis of nanoindentation data is non-trivial. It is suggested to pay particular attention to the following parts:

Screening of the dataset: The dataset should be thoroughly screened in the NanoPrepare software, and all unsuccessful curves should be removed before saving the cleaned dataset as a JSON file. Curves can still be excluded from the analysis in the NanoAnalysis software, but the JSON file cannot be changed. As such, to ensure consistency between the cleaned and analyzed dataset, it is suggested to carefully perform the screening process in the NanoPrepare software.

Filtering data: Using filters is useful when the data is noisy and recommended when performing the ES analysis. Three major filters are used as described below.

Prominency: This filter removes prominent peaks in the Fourier space, to eliminate instrumental oscillations typical of commercially available ferrule-top nanoindenters. The filter is based on three parameters: Prominency (a.u.): the peak prominency in the Fourier space; Minimum frequency (channels): the minimum frequency to be filtered; Band (% of peak position): the width around the filtered frequency in percentage of the peak position. Activate this filter

for data originating from commercially available ferrule-top nanoindenters by clicking on the checkbox and leaving default parameters.

Savitzky Golay (SAVGOL), algorithm from the SciPy library[34] (scipy.signal.savgol_filter): This filter smooths the data based on a local least-squares polynomial approximation. Activate this filter if the data is particularly noisy. Change the order of the polynomial and the filter window length in the GUI depending on how noisy the data is. For more details, see references[30,31]. Activate this filter for the ES analysis.

Median filter, algorithm from the SciPy library[34] (scipy.signal.medfilt): This filter smooths the data based on replacing each point with the median calculated around that point in a given window. Change the window length in the GUI depending on how noisy the data is. This filter is used as an alternative to the SAVGOL filter.

Activating the prominency filter helps remove instrumental noise (low-frequency oscillations) typical of commercial ferrule-top nanoindenters. In general, activating other filters such as the SAVGOL[34] when performing the simple Hertz analysis is not necessary. When computing the ES, it is recommended to activate both the prominency filter and the SAVGOL filter[34], with a smoothing window depending on the level of noise present in the data. This is because the ES contains a derivative term (equation 2), which is very sensitive to noise. For example, results in **Figure 7** were obtained using the prominency filter together with a SAVGOL filter[34] with window 80 nm and polynomial order 3. However, it is important not to over smooth the data, because this may hide any differences that are present between datasets.

CP identification: The most important part of the analysis is the identification of the CP, which strongly influences both the absolute value of E and its distribution[32,33]. Four algorithms based on automatic search procedures that locate the CP in order to remove human bias have been implemented in the NanoAnalysis software. All algorithms have been documented in the literature[32,33]. In general, every point in a region of interest is tested as a trial CP while an algorithm-specific parameter is being computed. The point that returns the optimized parameter, which can be its maximum or minimum value depending on the algorithm, is taken as the CP[32]. Those procedures have been implemented to remove human bias and take a statistical approach to the problem. Because each algorithm computes the CP based on the optimization of a given parameter, the identified CP will be slightly different for each algorithm. As such, it is paramount to maintain the same CP algorithm and specific parameters (e.g., window length for the RoV algorithm) between datasets that one wants to compare, as relative differences in E will be preserved. The different CP algorithms and their parameters are summarized below.

Goodness of Fit (GoF): An approach based on fitting a contact mechanics model (Hertz) from each *(z, F)* pair in a region of interest and selecting the fit having the highest R^2 value. It works well where the transition between non-contact and contact is evident, which happens with stiff materials such as highly crosslinked hydrogels. The algorithm is computationally expensive, and generally the slowest. Here, it has been implemented so that the Hertz model is only fitted up to a maximum δ of about 10% of R, as this has been shown to yield more accurate results[32].

Ratio of Variances (RoV): An approach based on computing the ratio of the variance of the deflection (force) signal in the non-contact and contact region[32].

Second derivative: An approach based on the second derivative of the deflection (force) signal[33]. It works well when the signal is clean. If the signal is too noisy, this approach is not recommended.

Threshold: An approach based on the average deflection (force) in the noncontact region[33]. In short, starting from a force value selected by the user near the contact region, the algorithm iterates through each point towards the baseline, until it finds the first point whose force value is larger than the average of the baseline. This point is selected as the CP. This algorithm is very robust and is the recommended one to use.

Details on how to use each algorithm are given below. The CP algorithms involve numerical constants that need to be changed in the GUI to suit the specific dataset. Specifically, the following parameters are common to the GoF, the RoV, and the Second Derivative method, allowing to select a sub-region of the curves (region of interest or ROI) where the CP will be searched for:

Safe threshold (nN): It defines the maximum force in nN (and the corresponding *z* point) from which the CP will be searched. This is the right boundary of the ROI, whose default value is 10 nN. All curves whose maximum force is below this threshold will be automatically moved to the failed set. Change this value to a force value slightly above the transition from non-contact to contact.

X range (nm): It defines the range in nm from the *z* point corresponding to the safe threshold. This is the left boundary of the ROI. The default of 1,000 nm is a good starting point, but if the CP is found too late in the curve (i.e., in the sloped region), increase this value. Conversely, if the CP is found too early (i.e., in the baseline), decrease this value.

Parameters specific to each algorithm are summarized here. For the GoF, the Window Fit (nm) represents the window in nm from the trial CP up to which the Hertz model is fitted. This is capped at a value of 10% of *R*. For the RoV, the Window RoV (nm) represents the window in nm to the left and right of the trial CP over which the variance of the deflection (force) signal is computed. For the second derivative, the Window P (nm) represents the window passed to the SAVGOL filter[34] used to compute the second derivative of the deflection (force) signal. Default values have been set from testing the different algorithms and it is generally not required to change them.

For the threshold algorithm, the following parameters can be changed:

Align threshold (nN): The force (F_0) from which the CP will be looked for starting from this point and moving toward the baseline. All curves whose maximum force is below this threshold will automatically be moved to the failed set. Its default value is 10 nN; however, change this value to a force value slightly above the transition from non-contact to contact. The corresponding *z* point (z_0) is stored for later use in the algorithm (see below).

Align left step (nm): This parameter defines the shift to add to the left of z_0 (default value 2,000 nm), which results in the calculation of a point defined by (z_0 - align left step). This point is the point around which the average of the baseline will be computed (see below).

Average area (nm): This parameter defines the average area to the left and right of (z_0 - align left step), over which the average of the baseline will be computed. Its default value is 100 nm, and it is not required to change it.

Iterating down from F_0, the CP is taken as the first point whose value is above the force defined by the average of the baseline.

Note on the ES and noise: The average ES may appear noisy at first with prominent sinusoidal oscillations, and as a result equation (3) may not fit correctly. If this is the case, increasing the window of the smoothing SAVGOL filter[34] usually solves this issue.

Modifications and troubleshooting of the method

Troubleshooting of the method

Wavelength scan troubleshooting

If an error message appears on the interferometer's display after performing the wavelength scan, the following problems may be the cause: i) The environment may be contaminated by noise. Get rid of any noise sources, including airflow, loud noises, and mechanical vibrations; ii) The probe may not be properly connected. Unplug and re-plug the green optical fiber connector; iii) The cantilever may be dirty. Clean it by submerging the probe in a Petri dish containing isopropanol for a few minutes, and then water; iv) An air bubble may be present on the cantilever. Submerge the probe in a Petri dish containing isopropanol and create some flow by pipetting the liquid up and down; v) The cantilever may be bent/stuck to the fiber, which can be seen under the microscope. Release it by gently touching the cantilever with a tissue wipe. Take extra care when touching the cantilever as the application of excessive force can break it; vi) The cantilever is missing from the probe, which can be seen under the microscope. The only solution is using a new probe. Try the wavelength scan again, which should now be successful.

Calibration troubleshooting

If calibration fails and the new factor is either NaN or is not in the expected range, the following problems may be the cause: i) The tip is not fully in contact with the substrate. Make sure the tip is in contact with the substrate by following the steps given in the **Protocol**; ii) Attractive forces between the tip and the glass surface (snap-on behavior) result in the calibration of the over-bended cantilever. Clean the probe by suberging it in isopropanol for 5 min, and then water. Clean the dish with isopropanol; iii) The tip/dish may be contaminated: Clean the probe by suberging it in isopropanol for 5 min, and then water. Clean the dish with isopropanol; iv) The cantilever may be bent/stuck to the fiber. Release it by gently touching it with a tissue wipe. Repeat both wavelength scan and calibration after troubleshooting.

Contact troubleshooting

If curves deviate from the shape shown in **Figure 4A**, experimental parameters need to be adjusted before continuing with the experiment. Two of the most common problems are:

An approach curve where the tip never enters contact with the sample (**Figure 4B**). This occurs when the contact threshold is set to a value that is too low, and noise causes the cantilever to bend by an amount corresponding to the given threshold. To solve this issue, navigate to the **Options** menu and slowly increase the threshold at steps of 0.01 and perform an indentation until the curve resembles the one shown in **Figure 4A**. Decreasing the speed in the same menu can also help solve this issue.

An approach curve where the tip started in contact with the sample (**Figure 4C**). This happens when the contact threshold is set to a value that is too high, and the cantilever does not bend by the amount corresponding to the given threshold when first touching the sample. To solve this issue,

slowly decrease the threshold in the **Options** menu at steps of 0.01 and perform an indentation until the curve resembles the one shown in **Figure 4A**. This issue is particularly problematic because the absence of a baseline prevents the correct computation of the CP, eventually leading to a miscalculation of *E*.

Modifications of the method

The protocol can be extended to quantify the *E* of different types of hydrogels. PAAm hydrogels were chosen for this protocol as they are the most common hydrogels used within the field of mechanobiology. However, the protocol is equally applicable to any type of elastic hydrogel[25], both synthetic, for example, polyethylene-glycol (PEG)[43] and gelatin methacryloyl (GelMA)[44,45]; and natural, such as collagen[46]. Moreover, there are no constraints on the dimensions of the sample to test, within reasonable limits. For example, this protocol has been used to quantify the *E* of synthetic PEG hydrogels that were later tested using a bulk rheometer and required to be ~15 mm in diameter and ~2 mm in thickness[8]. The protocol has also been implemented to characterize the *E* of PDMS membranes that were polymerized in a Petri dish (results not published).

Besides standard indentation of single cells performed using a conventional inverted phase-contrast microscope, ferrule-top nanoindenters are compatible with complex imaging systems and have been used to probe the local elasticity subcellular structures, such as the cell's nucleus and cytoplasm[47]. Whereas steps will need to be adjusted depending on the specific optical system, this protocol is of general applicability with respect to performing nanoindentation experiments and analyzing the resulting data.

Further, the protocol is not limited to measuring the mechanical properties of cells and hydrogels and can be adapted to measure the local elastic properties of more complex systems, including organoids[48], spheroids[49], and whole tissues such as kidneys, liver, spleen, and uterus[23]. The reader is directed to references[23,48,49] for specificities on performing nanoindentation experiments on such samples. One aspect to consider is that displacement control works in open-loop mode and does not receive feedback from the sample. As such, constant stress/strain and speed are not ensured, and softer parts of the sample will be indented more and faster as compared to stiffer regions. This is relevant for mechanically heterogeneous samples such as tissues, where it is more appropriate to choose either indentation control (I mode) or load control (P mode), ensuring a consistent stress/strain and speed across mechanically heterogeneous regions of the sample.

Limitations of the method

There is a growing body of evidence that viscoelasticity, in addition to elasticity, plays an important role in regulating physiologically and pathologically relevant processes. This is because cells, the ECM, and tissues are viscoelastic, and elasticity represents only one component of their mechanical behavior[50,51,52,53]. Whereas ferrule-top nanoindenters provide functionality for characterizing viscoelasticity, including stress relaxation, creep compliance, and dynamic mechanical analysis to extract both the storage and loss modulus over different frequency (time) regimes, this protocol only focuses on elasticity, which remains the most studied mechanical variable in the context of mechanobiology and tissue engineering (for example, see reference[3]).

The underlying assumption with consequences on both experiments and data analysis is that the indented substrate

behaves as a LEHI solid. This means that the stress-strain response is linear, there are no time-dependent behaviors, and the sample is mechanically homogeneous and isotropic. Based on these assumptions, the mechanical properties of the substrate are quantified through Young's modulus following a specific contact mechanics model, in this case, the Hertz model (equation 1). For small quasi-static forces/deformations, chemically crosslinked hydrogels such as PAAm gels used in this protocol[35] behave nearly as elastic solids and viscoelastic effects are minimal and negligible[53]. On the other hand, cells are not LEHI solids and show complex mechanical behavior[9]. The Young's modulus of cells is highly dependent on the strain rate (i.e., speed) of the indentation procedure, however, no clear trend is established and additional variables such as tip size and maximum indentation depth influence this relationship[9]. Nonetheless, for quasi-static deformations, such as those used in this protocol (v = 5 µm/s), cells show a marked elastic response and dissipative effects are minimal[9]. Strain rate dependency can be captured by more complex models taking into account time-dependent variables, to which the reader is referred to[54].

Further, following the same underlying assumption, the Poisson's ratio (v) is taken as 0.5 both in the Hertz and ES analysis. When comparing between samples, this only impacts results as a coefficient; however v has been shown to be a frequency-dependent quantity for cells[55] and to deviate from 0.5 for hydrogels[56].

Another limitation of the protocol lies in the fact that the software does not provide quantification of E through more sophisticated contact mechanics models. The Hertz model is the most used contact mechanics model in AFM experiments and it is extremely effective[13,15]; however, it does not take into account more complex events such as short- or long-range attractive forces between the tip and the sample. More complex models such as the Johnson-Kendall-Roberts model can capture these behaviors[13], but are not implemented in the software. For an overview of different contact mechanics models ranging in complexity, the reader is directed to reference[13].

Significance of the method with respect to existing/ alternative methods

The most common approach to quantify the local elastic properties of biomaterials and single cells at the microscale is AFM[13,14,15,16]. Despite being a powerful and versatile instrument, the AFM requires extensive training due to its complex setup before users can robustly perform experiments. Ferrule-top nanoindenters offer a plug-and-play solution while still allowing to apply nN forces with µm resolution to probe the local mechanical properties of biomaterials (e.g., references[8,19,20,21]). Whereas standardized protocols exist for the use of the AFM in the context of mechanobiology[16] and tissue engineering[14], there are no protocols detailing the operation of ferrule-top nanoindenter devices. This protocol allows an inexperienced user to perform nanoindentation experiments on both hydrogels and cells, by following guidelines that are intended to standardize the experimental workflow within the community. Further, data analysis of nanoindentation experiments is non-trivial and would remain largely inaccessible for users without experience in programming. Instructions are provided for the use of intuitive software that allows to clean and save the acquired dataset in light and standard format and perform both the standard Hertz analysis as well as the ES analysis[24] with a few clicks and in a reproducible way.

By following this protocol, results comparable with those obtained using the AFM are obtained, both for hydrogels' *E* (results in **Figure 6** compared to those in reference[35]) and cells' mechanical properties (results in **Figure 7** compared to those in reference[24]) at a fraction of the complexity. The method is of general applicability and can be adapted to different types of nanoindenters granted some steps are modified based on the specific device.

Importance and potential applications of the method in specific research areas

Characterizing the elastic properties of cells, hydrogels, and tissues is standard practice in many research labs focusing on mechanobiology, tissue engineering/regenerative medicine, and beyond[3]. This protocol can be used to quantify the elastic properties of single cells, hydrogels, and adapted for tissues and more complex biomaterials in the context of physiologically relevant processes marked by a change in mechanical properties. For example, to mimic the dynamics of the native ECM, it has been shown that degradable 3D PEG-laminin hydrogels allow cells to remodel their surrounding environment, leading to a decrease in the gels' *E* of ~50% over a period of 9 days as compared to the same gels without cells[21]. The protocol is of general applicability and is not restricted to the samples and optical setup described herein. It is envisaged that this protocol will facilitate the use of nanoindenters in research labs focusing on the study of mechanical properties in physiology and disease.

Disclosures

The authors have nothing to disclose.

Acknowledgments

GC and MAGO acknowledge all members of the CeMi. MSS acknowledges support *via* an EPSRC Programme Grant (EP/P001114/1).

GC: software (contribution to software development and algorithms), formal analysis (analysis of nanoindentation data), validation, Investigation (nanoindentation experiments on polyacrylamide gels), data curation, writing (original draft, review and editing), visualization (figures and graphs). **MAGO**: investigation (preparation of gels and cells samples, nanoindentation experiments on cells), writing (original draft, review and editing), visualization (figures and graphs). **NA**: validation, writing (review and editing). **IL**: software (contribution to software development and algorithms), validation, writing (review and editing); **MV**: conceptualization, software (design and development of original software and algorithms), validation, resources, writing (original draft, review and editing), supervision, project administration, funding acquisition **MSS**: resources, writing (review and editing), supervision, project administration, funding acquisition. All authors read and approved the final manuscript.

References

1. Dennis E. Discher, Paul Janmey, Y. W. Tissue cells feel and respond to the stiffness of their substrate. *Science.* **310** (5751), 1139-1143 (2005).
2. Roca-Cusachs, P., Conte, V., Trepat, X. Quantifying forces in cell biology. *Nature Cell Biology.* **19** (7), 742-751 (2017).
3. Guimarães, C. F., Gasperini, L., Marques, A. P., Reis, R. L. The stiffness of living tissues and its implications for tissue engineering. *Nature Reviews Materials.* **5**, 351-370 (2020).

4. Moeendarbary, E., Harris, A. R. Cell mechanics: Principles, practices, and prospects. *Wiley Interdisciplinary. Reviews Systems Biology and Medicine.* **6** (5), 371-388 (2014).
5. Butcher, D. T., Alliston, T., Weaver, V. M. A tense situation: Forcing tumour progression. *Nature Reviews Cancer.* **9** (2), 108-122 (2009).
6. Kubánková, M. et al. Physical phenotype of blood cells is altered in COVID-19. *Biophysical Journal.* **120** (14), 2838-2847 (2021).
7. Engler, A. J., Sen, S., Sweeney, H. L., Discher, D. E. Matrix elasticity directs stem cell lineage specification. *Cell.* **126**, 677-689 (2006).
8. Ciccone, G. et al. What caging force cells feel in 3D hydrogels: A rheological perspective. *Advanced Healthcare Materials.* **9** (17), e2000517 (2020).
9. Wu, P. H. et al. A comparison of methods to assess cell mechanical properties. *Nature Methods.* **15** (7), 491-498 (2018).
10. McKee, C. T., Last, J. A., Russell, P., Murphy, C. J. Indentation versus tensile measurements of young's modulus for soft biological tissues. *Tissue Engineering Part B Reviews.* **17** (3), 155-164 (2011).
11. Humphrey, J. D., Delange, S. L. *An Introduction to Biomechanics Solids and Fluids, Analysis and Design.* Springer-Verlag, New York. 271-371 (2004).
12. Prevedel, R., Diz-Muñoz, A., Ruocco, G., Antonacci, G. Brillouin microscopy: an emerging tool for mechanobiology. *Nature Methods.* **16** (10), 969-977 (2019).
13. Krieg, M. et al. Atomic force microscopy-based mechanobiology. *Nature Reviews Physics.* **1**, 41-57 (2019).
14. Norman, M. D. A., Ferreira, S. A., Jowett, G. M., Bozec, L., Gentleman, E. Measuring the elastic modulus of soft culture surfaces and three-dimensional hydrogels using atomic force microscopy. *Nature Protocols.* **16** (5), 2418-2449 (2021).
15. Gavara, N. A beginner's guide to atomic force microscopy probing for cell mechanics. *Microscopy Research and Technique.* **80** (1), 75-84 (2017).
16. Whitehead, A. J., Kirkland, N. J., Engler, A. J. Atomic force microscopy for live-cell and hydrogel measurement. *Methods in Molecular Biology (Clifton, N.J.).* **2299**, 217-226 (2021).
17. Chavan, D. et al. Ferrule-top nanoindenter: An optomechanical fiber sensor for nanoindentation. *The Review of Scientific Instruments.* **83** (11), 115110 (2012).
18. Van Hoorn, H., Kurniawan, N. A., Koenderink Ac, G. H., Iannuzzi, D. Local dynamic mechanical analysis for heterogeneous soft matter using ferrule-top indentation. *Soft Matter.* **12** (12), 3066-3073 (2016).
19. Baldini, F. et al. Biomechanics of cultured hepatic cells during different steatogenic hits. *Journal of the Mechanical Behavior of Biomedical Materials.* **97**, 296-305 (2019).
20. Emig, R. et al. Piezo1 channels contribute to the regulation of human atrial fibroblast mechanical properties and matrix stiffness sensing. *Cells.* **10** (3), 663 (2021).
21. Dobre, O. et al. A hydrogel platform that incorporates laminin isoforms for efficient presentation of growth

factors - Neural growth and osteogenesis. *Advanced Functional Materials.* **31** (21), 2010225 (2021).

22. Antonovaite, N., Beekmans, S. V., Hol, E. M., Wadman, W. J., Iannuzzi, D. Regional variations in stiffness in live mouse brain tissue determined by depth-controlled indentation mapping. *Scientific Reports.* **8** (1), 12517 (2018).
23. Wu, G., Gotthardt, M., Gollasch, M. Assessment of nanoindentation in stiffness measurement of soft biomaterials: kidney, liver, spleen and uterus. *Scientific Reports.* **10** (1), 18784 (2020).
24. Lüchtefeld, I. et al. Elasticity spectra as a tool to investigate actin cortex mechanics. *Journal of Nanobiotechnology.* **18** (1), 147 (2020).
25. Caliari, S. R., Burdick, J. A. A practical guide to hydrogels for cell culture. *Nature Methods.* **13** (5), 405-414 (2016).
26. Blumlein, A., Williams, N., McManus, J. J. The mechanical properties of individual cell spheroids. *Scientific Reports.* **7** (1), 7346 (2017).
27. Mirsandi, H. et al. Influence of wetting conditions on bubble formation from a submerged orifice. *Experiments in Fluids.* **61**, 83 (2020).
28. Vassalli, M., Ciccone, G. *CellMechLab/NanoPrepare: v0.1.1.* Zendo (2021).
29. Vassalli, M., Ciccone, G., Lüchtefeld, I. *CellMechLab/nanoindentation: v1.0.0.* Zendo (2021).
30. Savitzky, A., Golay, M. J. E. Smoothing and differentiation of data by simplified least squares procedures. *Analytical Chemistry.* **36** (8), 1627-1639 (1964).
31. Schafer, R. W. What is a savitzky-golay filter? in *IEEE Signal Processing Magazine.* **28** (4), 111-117 (2011).
32. Gavara, N. Combined strategies for optimal detection of the contact point in AFM force-indentation curves obtained on thin samples and adherent cells. *Scientific Reports.* **6**, 21267 (2016).
33. Lin, D. C., Dimitriadis, E. K., Horkay, F. Robust strategies for automated AFM force curve analysis-I. Non-adhesive indentation of soft, inhomogeneous materials. *Journal of Biomechanical Engineering.* **129** (3), 430-440 (2007).
34. Virtanen, P. et al. SciPy 1.0: fundamental algorithms for scientific computing in Python. *Nature Methods.* **17** (3), 261-272 (2020).
35. Tse, J. R., Engler, A. J. Preparation of hydrogel substrates with tunable mechanical properties. *Current Protocols in Cell Biology.* Chapter 10 (2010).
36. Pharr, G. M., Oliver, W. C., Brotzen, F. R. On the generality of the relationship among contact stiffness, contact area, and elastic modulus during indentation. *Journal of Materials Research.* **7** (3), 613-617 (1992).
37. Kumar, R., Saha, S., Sinha, B. Cell spread area and traction forces determine myosin-II-based cortex thickness regulation. *Biochimica et Biophysica Acta - Molecular Cell Research.* **1866** (12), 118516 (2019).
38. Kunda, P., Pelling, A. E., Liu, T., Baum, B. Moesin controls cortical rigidity, cell rounding, and spindle morphogenesis during mitosis. *Current Biology: CB.* **18** (2), 91-101 (2008).
39. Allen, M., Poggiali, D., Whitaker, K., Marshall, T. R., Kievit, R. A. Raincloud plots: a multi-platform tool for robust data visualization. *Wellcome Open Research.* **4**, 63 (2019).

40. Clark, A. G., Paluch, E. Mechanics and regulation of cell shape during the cell cycle. *Results and Problems in Cell Differentiation.* **53**, 31-73 (2011).

41. Langan, T. J., Rodgers, K. R., Chou, R. C. Synchronization of mammalian cell cultures by serum deprivation. *Methods in Molecular Biology (Clifton, N.J.).* **1524**, 97-105 (2017).

42. Hodgkinson, T. et al. The use of nanovibration to discover specific and potent bioactive metabolites that stimulate osteogenic differentiation in mesenchymal stem cells. *Science Advances.* **7** (9), eabb7921 (2021).

43. Kloxin, A. M., Kloxin, C. J., Bowman, C. N., Anseth, K. S. Mechanical properties of cellularly responsive hydrogels and their experimental determination. *Advanced Materials (Deerfield Beach, Fla.).* **22** (31), 3484-3494 (2010).

44. Loessner, D. et al. Functionalization, preparation and use of cell-laden gelatin methacryloyl-based hydrogels as modular tissue culture platforms. *Nature Protocols.* **11** (4), 727-746 (2016).

45. Yue, K. et al. Synthesis, properties, and biomedical applications of gelatin methacryloyl (GelMA) hydrogels. *Biomaterials.* **73**, 254-271 (2015).

46. Sarrigiannidis, S. O. et al. A tough act to follow: collagen hydrogel modifications to improve mechanical and growth factor loading capabilities. *Materials Today. Bio.* **10**, 100098 (2021).

47. Karoutas, A. et al. The NSL complex maintains nuclear architecture stability via lamin A/C acetylation. *Nature Cell Biology.* **21** (10), 1248-1260 (2019).

48. Ryu, H. et al. Transparent, compliant 3D mesostructures for precise evaluation of mechanical characteristics of organoids. *Advanced Materials (Deerfield Beach, Fla.).* **33** (25), e2100026 (2021).

49. Carvalho, D. T. O., Feijão, T., Neves, M. I., Da Silva, R. M. P., Barrias, C. C. Directed self-assembly of spheroids into modular vascular beds for engineering large tissue constructs Biofabrication Directed self-assembly of spheroids into modular vascular beds for engineering large tissue constructs. *Biofabrication.* **13** (3), 035008 (2021).

50. Chaudhuri, O., Cooper-White, J., Janmey, P. A., Mooney, D. J., Shenoy, V. B. Effects of extracellular matrix viscoelasticity on cellular behaviour. *Nature.* **584** (7822), 535-546 (2020).

51. Cantini, M., Donnelly, H., Dalby, M. J., Salmeron-Sanchez, M. The plot thickens: The emerging role of matrix viscosity in cell mechanotransduction. *Advanced Healthcare Materials.* **9** (8), e1901259 (2020).

52. Elosegui-Artola, A. The extracellular matrix viscoelasticity as a regulator of cell and tissue dynamics. *Current Opinion in Cell Biology.* **72**, 10-18 (2021).

53. Chaudhuri, O. Viscoelastic hydrogels for 3D cell culture. *Biomaterials Science.* **5** (8), 1480-1490 (2017).

54. Nguyen, T. D., Gu, Y. Determination of strain-rate-dependent mechanical behavior of living and fixed osteocytes and chondrocytes using atomic force microscopy and inverse finite element analysis. *Journal of Biomechanical Engineering.* **136** (10), 101004 (2014).

55. Mokbel, M., Hosseini, K., Aland, S., Fischer-Friedrich, E. The Poisson Ratio of the Cellular Actin Cortex Is Frequency Dependent. *Biophysical Journal.* **118** (8), 1968-1976 (2020).

56. Javanmardi, Y., Colin-York, H., Szita, N., Fritzsche, M., Moeendarbary, E. Quantifying cell-generated forces: Poisson's ratio matters. *Communications Physics.* **4**, 237 (2021).